Journal of
Plankton Research

plankt.oxfordjournals.org

J. Plankton Res. (2016) 38(2): 317–330. First published online October 27, 2015 doi:10.1093/plankt/fbv091

Costa Rica Dome: Flux and Zinc Experiments

Mesozooplankton biomass and grazing in the Costa Rica Dome: amplifying variability through the plankton food web

MOIRA DÉCIMA[1,5]*, MICHAEL R. LANDRY[1], MICHAEL R. STUKEL[2], LUCIA LOPEZ-LOPEZ[3] AND JEFFREY W. KRAUSE[4]

[1]SCRIPPS INSTITUTION OF OCEANOGRAPHY, 9500 GILMAN DR., LA JOLLA, CA 92093-0227, USA, [2]DEPARTMENT OF EARTH, OCEAN, AND ATMOSPHERI SCIENCE, FLORIDA STATE UNIVERSITY, TALLAHASEE, FL 32306, USA, [3]IEO CENTRO OCEANOGRAFICO DE SANTANDER, PROMONTORIO SAN MARTIN S/N, 39004 SANTANDER-CANTABRIA, SPAIN, [4]DAUPHIN ISLAND SEA LAB, 101 BIENVILLE BLVD, DAUPHIN ISLAND, AL 36528, USA AND [5]PRESENT ADDRESS: NATIONAL INSTITUTE OF WATER AND ATMOSPHERIC RESEARCH (NIWA), 301 EVANS BAY PARADE, HATAITAI 6021, WELLINGTON, NEW ZEALAND

*CORRESPONDING AUTHOR: moira.decima@niwa.co.nz

Received April 22, 2015; accepted September 24, 2015

Corresponding editor: Marja Koski

We investigated standing stocks and grazing rates of mesozooplankton assemblages in the Costa Rica Dome (CRD), an open-ocean upwelling ecosystem in the eastern tropical Pacific. While phytoplankton biomass in the CRD is dominated by picophytoplankton (<2-μm cells) with especially high concentrations of *Synechococcus* spp., we found high mesozooplankton biomass (~5 g dry weight m^{-2}) and grazing impact (12–50% integrated water column chlorophyll *a*), indicative of efficient food web transfer from primary producers to higher levels. In contrast to the relative uniformity in water-column chlorophyll *a* and mesozooplankton biomass, variability in herbivory was substantial, with lower rates in the central dome region and higher rates in areas offset from the dome center. While grazing rates were unrelated to total phytoplankton, correlations with cyanobacteria (negative) and biogenic SiO_2 production (positive) suggest that partitioning of primary production among phytoplankton sizes contributes to the variability observed in mesozooplankton metrics. We propose that advection of upwelled waters away from the dome center is accompanied by changes in mesozooplankton composition and grazing rates, reflecting small changes within the primary producers. Small changes within the phytoplankton community resulting in large changes in the mesozooplankton suggest that the variability in lower trophic level dynamics was effectively amplified through the food web.

KEYWORDS: trophic transfer; food chain; efficiency; OMZ; secondary production

INTRODUCTION

The Costa Rica Dome (CRD) is an open-ocean upwelling ecosystem in the eastern tropical Pacific (ETP) that develops seasonally off the coast of Central America in the area of 9°N, 90°W (Fig. 1). Ekman pumping in the CRD region is forced by a coastal wind jet from the northeast in winter and southwesterly winds from the Intertropical Convergence Zone in summer (Fiedler and Talley, 2006). Seasonally, the wind transition results in a shift in position of the eastern shoaling of the thermocline ridge associated with the North Equatorial Counter Current (NECC), which resides near the coast during winter and migrates several 100 km offshore to form the CRD during summer. Offshore upwelling in the CRD, separated from the coast, becomes distinctly visible in satellite images of sea surface cooling and elevated chlorophyll (Chl *a*) between June and August (Fiedler, 2002).

Enhanced primary production suggested by the high Chl *a* in satellite images of the CRD (Pennington *et al.*, 2006) is accompanied by uniquely high concentrations of *Synechococcus*, exceeding 10^6 cells mL^{-1} (Fiedler, 2002; Saito *et al.*, 2005). Productivity of the CRD is further believed to be trace-metal limited, suppressing diatoms (Franck *et al.*, 2005) and blooms of larger phytoplankton cells that typically characterize upwelling features. Nonetheless, the region enigmatically appears to support high standing stocks of zooplankton (Blackburn *et al.*, 1970; Sameoto, 1986; Fernandez-Alamo and Farber-Lorda, 2006), as well as high abundances of seabirds and cetaceans that exploit the CRD as a feeding ground (Ballance *et al.*, 2006; Vilchis *et al.*, 2006), and tuna (Green, 1967; Scott and Cattanach, 1998). It remains a mystery how lower trophic levels of this unusual picophytoplankton-dominated system function to sustain high stocks of larger animals due to the lack of rate measurements and trophic studies within the region. Because of these highly unusual conditions, the CRD represents a unique opportunity to investigate mechanisms shaping food web relationships between phytoplankton and mesozooplankton.

In this study, conducted as part of the CRD FLUx and Zinc Experiments (FLUZiE) cruise in July 2010, we investigated biomass, size-structure, composition and grazing of mesozooplankton (net-collected animals >200 μm) during five Lagrangian experimental studies of production and food web interactions in the CRD region. Our goals were to quantify the roles of mesozooplankton in the pelagic food web and to explore relationships that might explain variability in trophic fluxes and efficiency within the region. We highlight potentially important changes that occur among size-class partitioning of primary production, zooplankton size-structure and taxonomic composition as pelagic communities evolve in waters advected from the central upwelling dome region to outer areas.

METHOD

The CRD FLUZiE cruise was conducted from 22 June to 25 July 2010, in the area of 7.5–10.2°N, 87–93°W onboard the "R/V Melville." In this paper, we present results from five Lagrangian experiments, called "cycles," in which we conducted daily rate and standing stock assessments while following water parcels marked by a satellite-tracked drifter with a holey-sock drogue center at 15 m. Full details of the experimental design are provided in the introduction to this issue (Landry *et al.*, 2016a).

Mesozooplankton collection

Double-oblique tows in the upper euphotic zone were taken twice daily to obtain estimates of mesozooplankton standing stocks and grazing on phytoplankton. We sampled between 1000 and 1300 h and between 2100 and 2400 h to capture daytime and nighttime communities. Our 1-m ring net had 202-μm Nitex mesh and was equipped with a General Oceanics flow meter to record volume filtered and a Vemco depth logger to record the depth of the tow. We conducted a total of 41 tows over the 5 different cycle experiments. The average tow depth was 154 ± 3 m [mean $\pm$ standard error of the mean (SE)] and volume filtered was 329 ± 17 m^3. This depth was well within the euphotic zone, which was typically very shallow, in the upper 50 m of the water column (Selph *et al.*, 2016).

The net was washed down with seawater upon retrieval on deck, and organisms were immediately anesthetized with carbon dioxide in soda water to prevent gut-content evacuation (Kleppel and Pieper, 1984). The samples were quickly divided with a Folsom splitter, and typically half was preserved in 4% buffered formalin solution, and the other half was split further for biomass and gut-content analyses. Because of the large amounts of material collected, we usually analyzed only 1/4 of the total sample, 1/8 for biomass and 1/8 for gut pigments, the latter done first to minimize pigment degradation. Samples for both analyses were size-fractionated using nested sieves into five size classes of 0.2–0.5, 0.5–1, 1–2, 2–5 and >5 mm.

Biomass estimates

Size-fractionated samples were concentrated onto pre-weighed Nitex filters, rinsed in ammonium formate, placed in petri dishes and frozen at −80°C for later analyses. On land, the samples were thawed and dried at

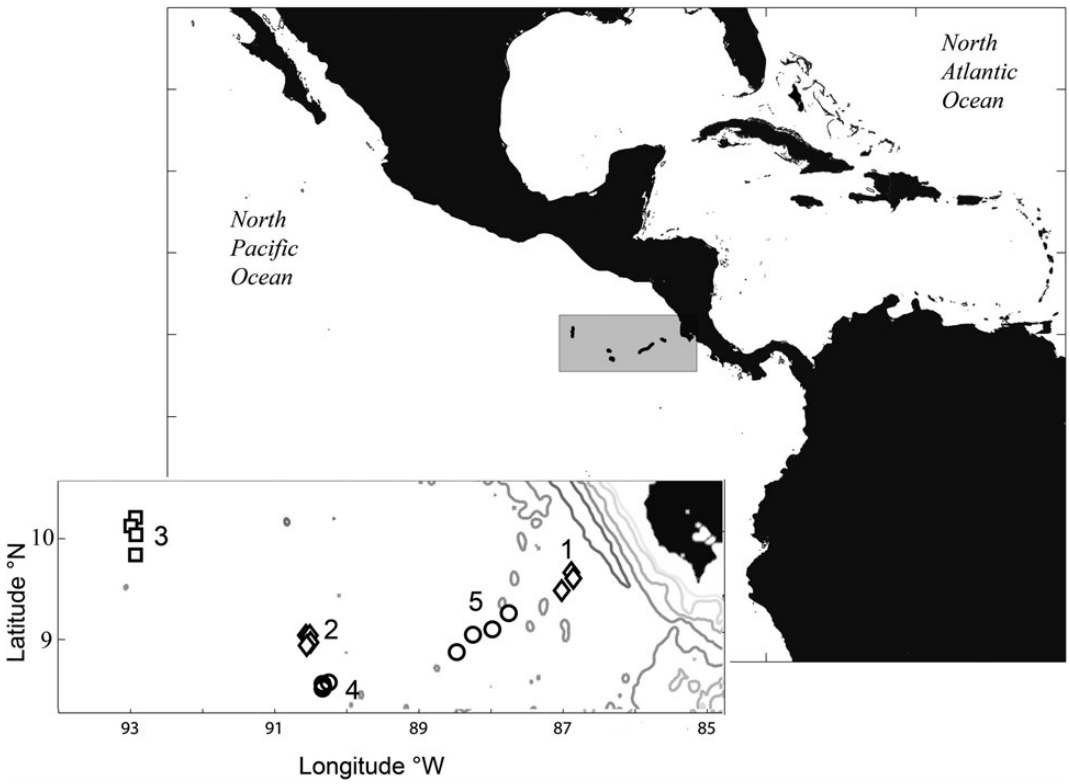

Fig. 1. Map of experimental cycles in and around the Costa Rica Dome (CRD). Large map shows the position of the CRD with respect to continental landmass, smaller inset shows the separate areas of our experimental cycles, which are numbered as in the text. Cycle 2 and 4 are located in the center of the dome area. Individual points represent different sampling days within cycles.

60°C for 24 h, and weighed at room temperature to an accuracy of 0.01 mg (Denver Instrument). Dry weight was calculated by subtracting the initial Nitex filter weight and multiplying by appropriate split factors. Areal estimates of g DW m^{-2} were obtained by multiplying by the tow depth and dividing by volume filtered. Daily average areal estimates are only reported for day/night pairs. Migrant biomass estimates were obtained by taking the difference between day and night paired tows within each experimental day and cycle.

Grazing estimates

Each size-fraction was concentrated onto a Nitex filter, placed in a petri dish and frozen in liquid nitrogen. The largest size-fraction (>5 mm) was typically analyzed whole; all other sizes were subsampled and analyzed in duplicate. For grazing estimates based on chlorophyll *a* (Chl *a*), we subsampled 1/8 (0.2, 0.5 and 1-mm size classes) or 1/4−1/2 (2-mm size class) of the filter with a razor blade, added to a test tube with 7 mL of 90% acetone and sonicated with an ultrasonic tissue homogenizer. Test tubes were kept on ice before and after this process, and samples were allowed to sit in the dark at −20°C for 2−4 h for Chl *a* extraction. Samples were then centrifuged at 3000 g for 5 min to remove zooplankton particles, and poured into 7-mL borosilicate glass tubes for fluorometric analysis. Chl *a* and phaeopigments (Phaeo) were analyzed using a 10 AU Turner fluorometer with a Chl *a* filter set, before and after acidification with 2 drops of 10% HCl.

We did not multiply our Phaeo estimates by any factors to correct for pigment degradation because conversion to non-fluorescent products is inherently taken into account in experimental determinations of gut clearance rates (Durbin and Campbell, 2007). We used a gut passage rate of 2.1 h^{-1}, which was measured under similar surface temperatures and Chl *a* values in the equatorial Pacific (Zhang *et al.*, 1995). We choose this rate instead of using the general temperature relationship, $K\,(\mathrm{min}^{-1}) = 0.0124\ e^{0.07675\ T\ (^{\circ}C)}$ (Dam and Peterson, 1988), because the relationship was derived for polar and temperate zooplankton in the temperature range of −1−20°C. We computed water-column integrated estimates of Chl *a* consumption by multiplying tow gut Phaeo estimates by the tow depth and dividing by volume filtered. Although Chl *a* is also found in the foreguts of mesozooplankton grazers (Conover *et al.*, 1986), we only used the Phaeo

estimates to minimize bias from phytoplankton aggregates that may have been caught in our net. Finally, phytoplankton standing stocks were depth-integrated using the trapezoidal method (Taylor *et al.*, 2016), from which we calculated the percentage of water-column Chl *a* consumed by the mesozooplankton.

To assess the grazing variability on *Synechococcus* in the different water parcels examined, we analyzed one day/night pair per cycle for phycoerythrin (PE). Samples were washed from filters with glycerol saline solution, ground with a tissue homogenizer to release gut contents and centrifuged to separate mesozooplankton tissues. After refrigeration for 2–24 h, fluorescence was measured on a Turner Designs TD-700 fluorometer with a PE filter set (Wyman, 1992; Dore *et al.*, 2002). In addition, we conducted 7 net tows using a 100-μm mesh net, with similar tow specifics (depth, volume filtered and length of tow) as our standard 202-μm mesh net. These tows were not evenly distributed among cycles, and results are presented here only to illustrate the size-structure of mesozooplankton grazing on PE. Inter-cycle variability was evaluated with the 202-μm mesh tows, as most grazing was done by the larger organisms.

Spectral slopes

Patterns in community size-composition were investigated by fitting spectral slopes to the size-fractionated biomass and grazing results, following the equation:

$$\log\left(\frac{Bx}{\Delta x}\right) = m \times [\log(x)] + b$$

where Bx is the DW of the sample retained on a mesh size x, Δx is the size of the interval for each size class (0.303, 0.495, 1, 3 and 5 mm in this case) and m and b correspond to the parameters of the linear best fit line, the slope and the y-intercept, respectively. The line was typically determined by the 5 size-fraction data points, although on a few occasions the >5-mm size class was empty and we calculated the line based on only 4 points. The R^2 values were investigated to ensure a goodness of fit. Most values, 36 of the 41 cycle tows, had R^2 values >0.8. The size-fractionated values for the other five tows were inspected. Usually, the lower R^2 value occurred when there was a greater-than-normal amount of material in the >5-mm size class, due to gelatinous organisms, thus decreasing both the spectral slope and the goodness of fit. However, we kept these values because they captured community changes that could be important. As these cases were also evenly distributed among cycles, they did not significantly affect our inter-cycle comparisons. We only report the nighttime spectral slopes because night sampling is more representative of the whole zooplankton community, which includes organisms undergoing diel vertical migration (DVM). Biomass estimates from both day and night tows are also presented separately in our Results.

Zooplankton composition

To shed further light on the drivers of variability among cycles, one day and one night tow from each cycle were chosen for enumeration of the main groups of zooplankton. Copepods, euphausiids, ostracods, appendicularians, doliolids and salps were counted and measured for biomass and abundance estimates. Typically, 1/16 of the sample was enumerated for euphausiids, ostracods, doliolids and salps, and 1/10 of that fraction was analyzed for appendicularians and copepods. Samples in formalin were split three times using a Folsom splitter, and the subsample was transferred to filtered seawater. For copepods and appendicularians, we used a Stempel pipette to take 10% of the sample volume, carefully suspending animals before sampling. These were then sorted under a Zeiss stereomicroscope, and specimens pulled out and archived for later imaging. Euphausiids were the only organisms identified to species level, the remaining were only identified to group level (not presented here). All organisms were later counted and imaged using an Imaging Development Systems mounted camera with a USB connection to a computer running Microsoft XP. Images were saved as .jpg and animals were measured using the program Image J.

All data were analyzed using Matlab R2007 and the included statistical packages. Because the variability in ecological and plankton data was substantial, we used the *P*-value of 0.1 as the level denoting significance, as have others investigating zooplankton patterns in open-ocean environments (e.g. Zhang *et al.*, 1995).

RESULTS

CRD characteristics

Hydrography and water-column characteristics of the CRD during our experimental study are described in detail elsewhere in this volume (Landry *et al.*, 2016a; Selph *et al.*, 2016). Briefly, the center of the CRD was located using a combination of satellite images and ADCP mapping prior to Cycles 2–5. Cycle 1 was the most coastal of our experiments. Cycle 2 was situated closest to the center of the shoaled isopycnals (Fig. 1, Landry *et al.*, 2016a). We left a disposable drifter in this water parcel to locate and resample it later (Cycle 4). Cycle 3 was carried out on the outer northwest edge of

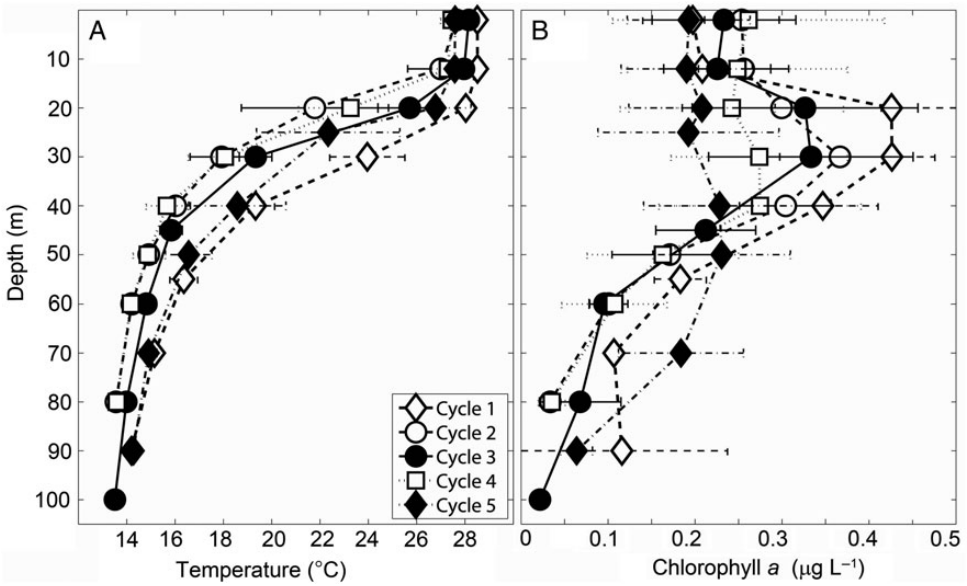

Fig. 2. Water-column profiles for experimental Cycles 1–5. Average ± SD of multiple days for each cycle. (**A**) Temperature and (**B**) chlorophyll *a* profiles.

the dome area. Cycle 4 was done in the central dome area, in waters downstream of Cycle 2 (position of drifter released after Cycle 2). Finally, Cycle 5 was east of the CRD core, in waters in the NECC flowing rapidly toward the Costa Rica coast (Fig. 1).

Despite the wide area covered, water-column characteristics of the five cycles were relatively similar (Fig. 2). A very strong thermocline separated a shallow mixed layer (12–30 m) from waters typically 10–12°C colder by 50 m depth, and this was present in all cycles (Fig. 2A). Subtle differences in temperature were apparent in the thermocline: Cycle 1 had the warmest waters, Cycles 2 and 4 were the coldest and Cycles 3 and 5 were intermediate (Fig. 2A). Chl *a* concentrations below the mixed layer were fairly similar. The warmer coastal waters of Cycle 1 had higher peaks, followed by Cycles 2–4, and Cycle 5 had the lowest Chl *a* concentration in the upper water column (Fig. 2B). Integrated Chl *a* values were very similar for Cycles 2–5, ranging between 15 and 18 mg Chl *a* m^{-2}, and only reached ~22 mg Chl *a* m^{-2} during Cycle 1 (Taylor *et al.*, 2016).

Mesozooplankton biomass and grazing

Average day/night biomass was remarkably similar among cycles, with a regional average of 5.2 ± 0.2 g m^{-2} (mean ± SE, Table I) and no statistical differences among cycles [analysis of variance (ANOVA), $P > 0.1$]. Biomass spectral slopes, which give a measure of size composition, were different among the five cycles, but the differences were subtle and statistical significance was limited due to high intra-cycle variability (Table I). Cycle 2 was dominated more by larger animals and Cycle 5 by smaller organisms (ANOVA, $P < 0.1$; Table I). The variability in size-class and day/night contributions not captured by the average values can be seen more clearly in Fig. 3A. The standing stocks were similar, but the DVM community showed more notable variability among cycles (Fig. 3A), with higher nighttime biomass in Cycles 2–4 (Table I).

Table I: Average (mean ± SE) day/night mesozooplankton biomass (g m^{-2}), spectral slopes (dimensionless), grazing (mg Chl a m^{-2} day^{-1}) and migrants (night − day biomass) for each cycle

Cycle	Dry weight (g m^{-2})	Spectral slopes (nighttime)	Grazing (g Chl *a* m^{-2} day^{-1})	Migrants (g m^{-2})
1	4.86 ± 0.56	−1.27 ± 0.13	3.53 ± 0.73	0.13 ± 0.70
2	5.05 ± 0.22	−1.14 ± 0.07	1.82 ± 0.13	3.88 ± 0.84
3	5.40 ± 0.88	−1.45 ± 0.05	7.01 ± 0.95	2.99 ± 2.02
4	5.37 ± 0.19	−1.25 ± 0.11	3.05 ± 0.59	4.31 ± 1.49
5	5.18 ± 0.52	−1.50 ± 0.10	7.01 ± 0.61	2.61 ± 1.00

Cycles 2–5 each involved 4 experimental days; Cycle 1 was 3 days.

In contrast to the regional uniformity of Chl *a* concentrations and areal mesozooplankton biomass, grazing was highly variable among cycles (Table I, Fig. 3B). Cycles 3 and 5 were significantly higher than Cycles 2 and 4 (one-way ANOVA, $P < 0.05$), whereas Cycle 1 was not significantly different from any other location (Table I). There was clear diel variability in grazing, with higher grazing in the nighttime (Fig. 3B). The main

contributors to grazing were the smallest size classes (0.2–2 mm), responsible as a regional average for 90.7 ± 4.8% (mean, SE), but the 2–5 mm size classes also contributed substantially in Cycles 3 and 5. Grazing was therefore not correlated with total community biomass (Fig. 4A). However, grazing was negatively related to spectral slopes; higher grazing occurred when the size-structure was skewed toward smaller organisms (Fig. 4B).

We were able to measure grazing on *Synechococcus* during every cycle, but this was only 0.6–4.5% of the integrated population standing stocks (Table II), with no significant differences among cycles. Estimates of percent PE standing stock consumed (% PE) followed a pattern similar to that for grazing on Chl *a* (Table II). The results from the tows made with the 100-μm mesh net were analyzed to ascertain if the size-fractionated patterns were always greatest for the smallest organisms. Notably, the 100–200 μm size class had low PE concentrations, suggesting that the source of PE was not small aggregates caught in the net mesh (Table III). Most grazing was done by organisms between 0.2 and 2 mm in size, accounting for ~75% of PE consumption.

Diel migrants

Patterns in DVM can be observed from the day/night difference in biomass of the 5 size-classes (3A). Cycles 2,

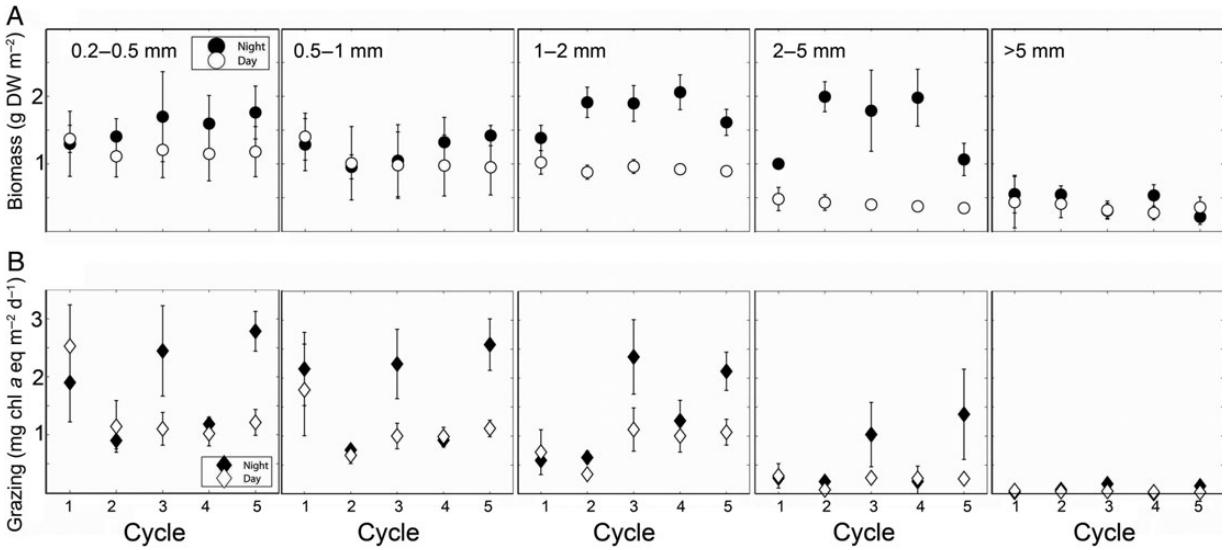

Fig. 3. Size-structured day and night (**A**) biomass (g DW m^{-2}) and (**B**) grazing (mg Chl *a* m^{-2} day^{-1}) for every cycle by size class. Cycle 2 and 4 are characterized as 'dome cycles' and Cycles 3 and 5 are located at the edge of the dome, whereas Cycle 1 is located more coastally. Estimates are per m^{-2} for the upper 150 m of the water column.

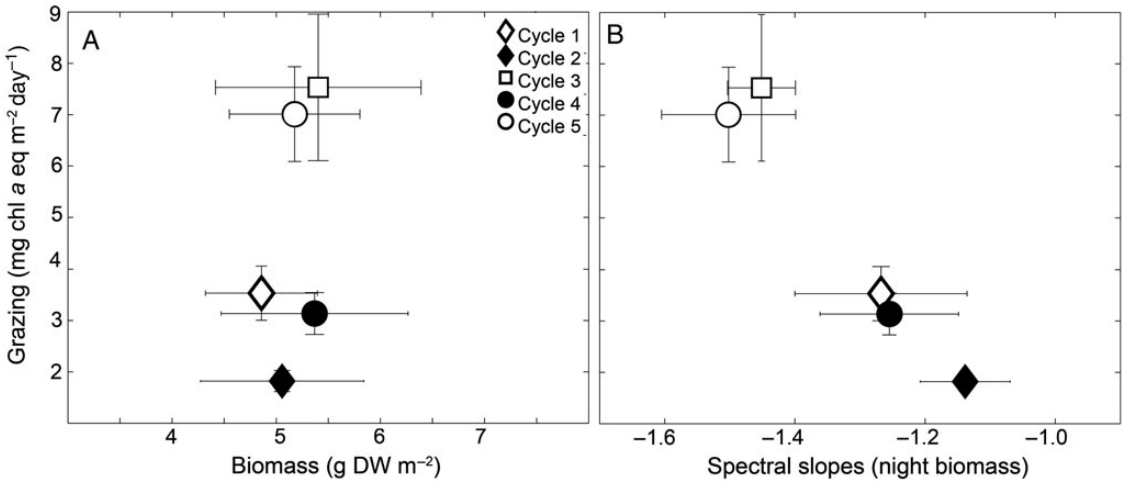

Fig. 4. Averages (± SE) grazing (mg Chl *a* equivalents m^{-2} day^{-1}) as a function of (**A**) mesozooplankton dry weight (g m^{-2}), and (**B**) nighttime biomass spectral slopes. Estimates are per m^{-2} for the upper 150 m of the water column.

Table II: Average (mean ± SE) day/night grazing on Synechococcus *(cells m^{-2} day^{-1}), percent (%) water column based on phycoerythrin (PE), percent water column phytoplankton grazed (% Chl* a*), % zooplankton body carbon from PE and % zooplankton body carbon from Chl* a *for experimental cycles 1–5*

Cycle	*Synechococcus* (cells m^{-2} day^{-1})	PE (% Syn standing stock)	Chl *a* (% standing stock)	% Body carbon from PE	% Body carbon from Chl *a*
1	$6.02 \times 10^{10} \pm 2.95 \times 10^{10}$	1.7 ± 0.8	16.5 ± 3.5	0.31 ± 0.15	15.3 ± 2.1
2	$4.24 \times 10^{10} \pm 1.85 \times 10^{10}$	0.6 ± 0.3	10.4 ± 0.8	0.21 ± 0.09	8.4 ± 0.5
3	$5.67 \times 10^{10} \pm 1.53 \times 10^{10}$	2.6 ± 07	43.9 ± 9.1	0.26 ± 0.07	31.9 ± 4.8
4	$3.55 \times 10^{10} \pm 2.2 \times 10^{10}$	1.1 ± 0.7	20.5 ± 3.9	0.17 ± 0.1	14.6 ± 1.9
5	$3.76 \times 10^{10} \pm 9.26 \times 10^{9}$	4.5 ± 1.1	41.6 ± 3.6	0.18 ± 0.05	30.2 ± 3.9

Table III: Average (± SE) contribution of each size class to grazing on phycoerythrin (PE) and chlorophyll a *(Chl* a*)*

Size class (mm)	% Total PE grazed	% Total Chl *a* grazed
0.1	6.5 ± 1.7	ND
0.2	23.3 ± 4.5	32.1 ± 1.7
0.5	20.3 ± 3.5	30.0 ± 1.2
1	32.4 ± 8.5	28.5 ± 1.9
2	17.4 ± 5.6	8.1 ± 1.2
>5	ND	1.3 ± 0.3

ND: no data.

3 and 4 group together, showing increasing DVM with size fractions, from 0.5 to 2 mm, and a decrease in the >5-mm class (Fig. 5, Table IV). The decrease in the >5-mm size class should be interpreted with caution, since this size is not quantitatively sampled with the 1-m ring net. Cycles 1 and 5 had similar patterns among the size classes, with low night biomass in the 1 and 2 mm sizes (Fig. 3A). Total migrant biomass closest to shore in Cycle 1 was not significantly different from zero, with higher abundances in the daytime for animals <1 mm and no diel difference for organisms >5 mm (Table I, Fig. 3A).

Zooplankton taxonomic composition

Significant variability in taxon contributions to the zooplankton community was found among cycles (Table IV, Fig. 5). Copepod abundance was highest in Cycle 1 and lowest in Cycle 2, whereas Cycles 3–5 were similar (Fig. 5). Euphausiid abundance was notably higher during Cycle 2 (Table IV). Ostracods were similar among all cycles, except for Cycle 3, which had significantly higher numbers (ANOVA, $P < 0.05$). Interestingly, Cycle 3 also had significantly higher abundances of doliolids. Appendicularians, known for making significant contributions to grazing on smaller phytoplankton, were highest in Cycle 1 (relatively low grazing) and Cycle 5 (high grazing). Cycle 2 had very low abundances, whereas appendicularian abundances for Cycle 3 and 4 were intermediate. Cycle 5 was the only one to have significant numbers of salps in the regular net tows, observed in the daytime sample (Fig. 5). The euphausiids were also the only group to show a clear difference in day and night abundance, with higher values at night (Table IV).

Grazing vs. production

We investigated the relationship between grazing and various measurements for the phytoplankton community. Grazing showed no relationship with either integrated or peak Chl *a* concentrations (Fig. 6A and B). Lower integrated and peak Chl *a* concentrations were found in Cycles 2, 3 and 5, but these differences were not significant. Grazing variability was also not related to new production (Fig. 6C). While Cycle 5 did have high grazing and the highest new production, Cycle 3 was the lowest of the oceanic cycles in terms of nitrate uptake (Stukel *et al.*, 2016), but similar in grazing magnitude to Cycle 5 (Fig. 6C). Percent diatom contribution to new production was also only marginally related to grazing variability.

We converted Chl-based grazing into carbon equivalent rates using a regional water column integrated C:Chl ratio of 76 (Stukel *et al.*, 2013; Taylor *et al.*, 2016). These rates were negatively related to estimates of cyanobacteria production, which come from biomass and growth rates of picophytoplankton populations determined daily from depth profiles of *in situ* incubated dilution experiments, analyzed by flow cytometry (Landry *et al.*, 2016b). Figure 7A shows this negative relationship for *Synechococcus* spp., and a similar relationship also occurs for *Prochlorococcus* spp. (not shown). Additionally, grazing was positively correlated with biogenic silica production, a measure of diatom production (Fig. 7B).

By subtracting picophytoplankton production (determined by flow cytometry) from ^{14}C-uptake total primary production, we estimated the production of phytoplankton >2 μm. The resulting production of nano- and microphytoplankton was sufficient to sustain mesozooplankton

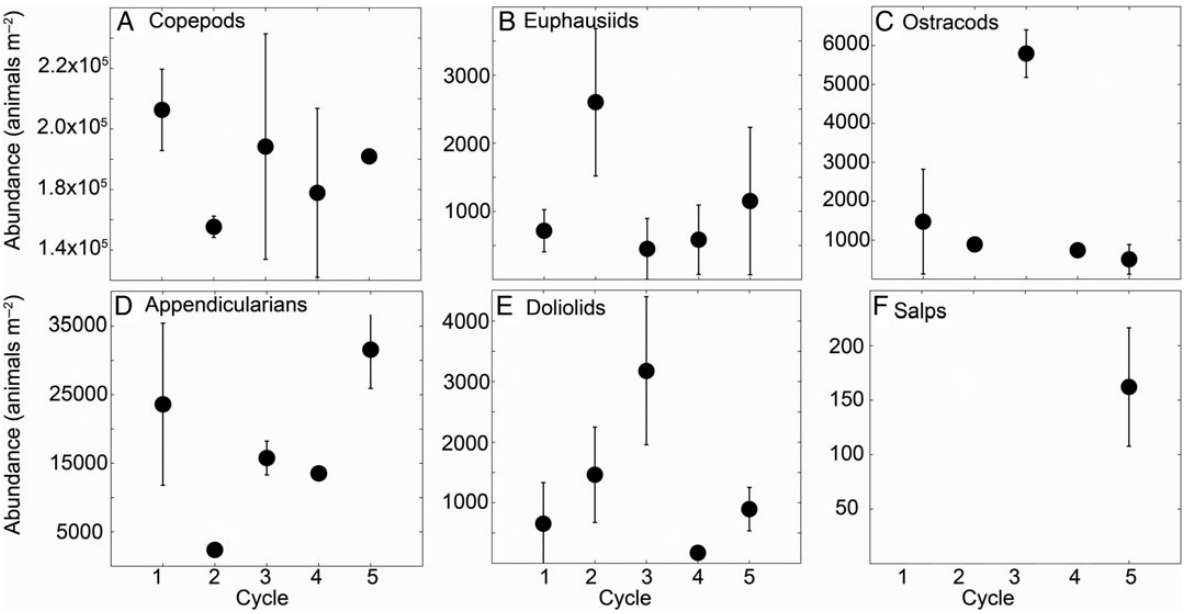

Fig. 5. Taxonomic contributions of major mesozooplankton groups to net collections during experimental cycles 1–5. Averages ± SD of day/night pair. Some points on the graph have error bars not large enough to be visible, see Table IV for exact values of each enumerated tow.

Table IV: Mesozooplankton functional group abundances for one day and one night tow analyzed per cycle

	Euphausiids		Appendicularians		Doliolids		Ostracods		Copepods		Salps	
	Day	Night	Day	Night	Day	Night	Day	Night	Day	Night	Day	Night
1	405	1024	31 961	15 257	1133	174	2427	523	2.51×10^5	2.14×10^5	0	0
2	1520	3684	2991	1761	2019	906	922	861	1.50×10^5	1.60×10^5	0	0
3	0	897	17 517	14 018	2315	4037	5362	6224	2.61×10^5	1.56×10^5	0	0
4	76	1093	12 892	14 161	114	231	683	800	1.38×10^5	2.17×10^5	0	0
5	71	2234	27 563	35 578	1148	640	236	775	2.05×10^5	1.99×10^5	200	0

grazing for all cycles (Fig. 7C), as they all fall below the 1:1 line (there are no data for Cycle 1 because ^{14}C incubations were not done). Not surprisingly, the Cycle furthest from the 1:1 line was Cycle 2, with large phytoplankton produced in significant excess over grazing (Fig. 7C). The negative correlation with small phytoplankton coupled with the positive relationship with large phytoplankton in some cycles suggests that regional variability in mesozooplankton grazing is related to variability in phytoplankton size-class partitioning of primary production.

DISCUSSION

Methodological considerations

High mesozooplankton grazing within the CRD region may be somewhat surprising given the dominance of picophytoplankton, which comprised more than half of total phytoplankton carbon biomass during our cruise (Taylor *et al.*, 2016). Because phytoplankton can get trapped in the net-collected samples that we used to assess community gut pigment contents, we only took Phaeo into account for our grazing estimates (ignoring the chlorophyll contribution). This keeps our estimates conservative in that regard, since it is well documented that Chl *a* is found in both zooplankton guts and fecal pellets (Shuman and Lorenzen, 1975). Low phytoplankton contamination of the gut pigment estimates is also suggested by our PE grazing results, which showed very low amounts of PE in the smallest 100- to 200-μm size-fraction (Table III). Another potential source of error with our approach includes the gut passage time. This constant was derived for copepods and is used generally for crustaceans (Dam and Peterson, 1988; Zhang *et al.*, 1995). The few estimates for appendicularians (the other abundant mesozooplankton grazers) that we are aware of were done in polar waters (0–1°C), and gut passage times were 45–104 min (Bochdansky *et al.*, 1998; Acuna

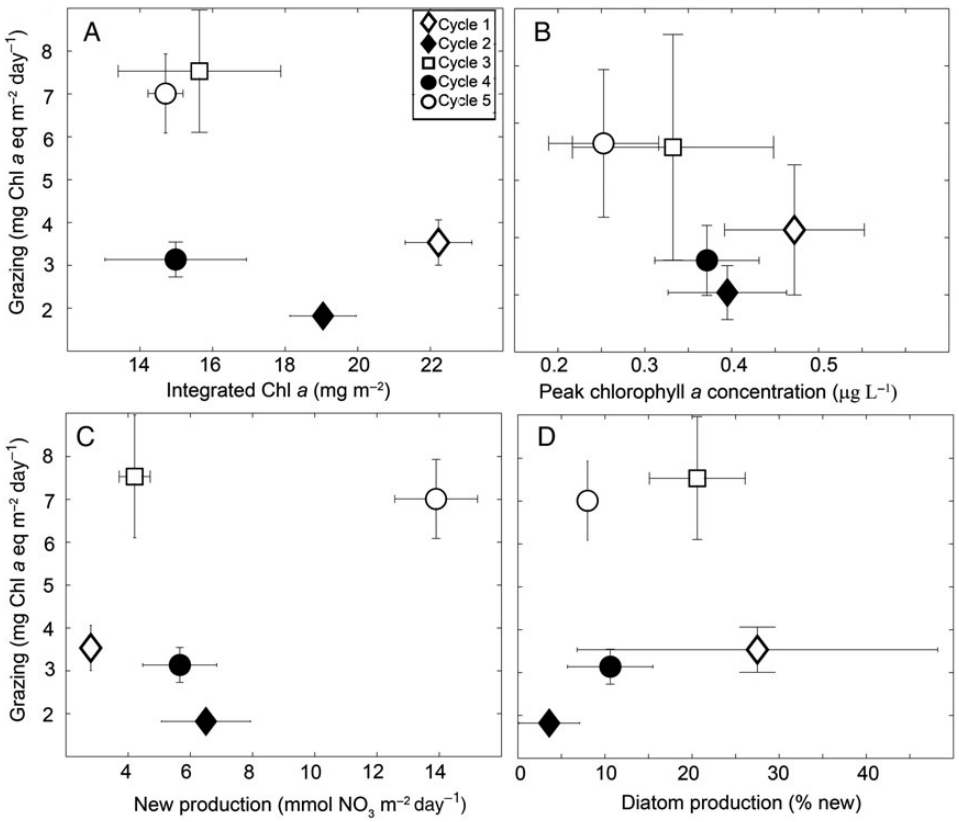

Fig. 6. Grazing (mg Chl *a* equivalents m^{-2} day^{-1}) as functions of (**A**) integrated Chl *a* (mg m^{-2}), (**B**) peak Chl *a* concentration (μg L^{-1}); (**C**) new production (mmol NO_3^- day^{-1}) and (**D**) diatom production (% new production). Averages ± SE.

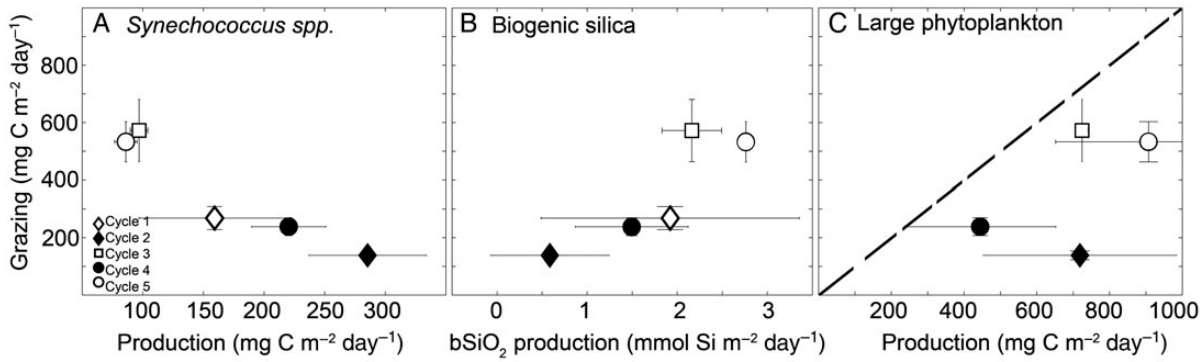

Fig. 7. Grazing (mg C m^{-2} day^{-1}) versus production relationships for: (**A**) *Synechococcus* production (mg C m^{-2} day^{-1}), (**B**) net biogenic silica production (mmol Si m^{-2} day^{-1}) and (**C**) larger phytoplankton production (mg C m^{-2} day^{-1}). Points are average ± SE. Line marks 1:1 relationship.

et al., 2002). The estimate for copepods at the same temperature falls within the same range: 74 min based on Dam and Peterson (Dam and Peterson, 1988). The similarity in these two rates in cold waters and the tendency for metabolic rates to scale with temperature would suggest that we are at least conservative in our grazing estimates, given that pelagic tunicates typically have higher metabolic rates than copepods (Bone, 2003). If, however, clearance rates for appendicularians scaled faster with temperature than for copepods and this effect was driving our conclusions, the abundance patterns would suggest that the cycles with highest grazing would be Cycles 1 and 5, with Cycles 3 and 4 exhibiting similar rates, which is not the pattern we observed. We therefore feel confident in our general use of one temperature-dependent constant for the community.

Mesozooplankton community

The qualities of the CRD mesozooplankton community are consistent with upwelling systems in general, characterized by high standing stocks and efficient transfer of carbon from phytoplankton to mesozooplankton. Biomass at the time of our study was high, comparable to estimates from past cruises (Sameoto, 1986). We only sampled the upper ~150 m, but past studies on the vertically stratified distribution of zooplankton showed that most of the biomass in this region is concentrated in the upper water column (Longhurst, 1985; Sameoto, 1986; Wishner *et al.*, 2013), and this was confirmed in our study as well (Jackson and Smith, 2016). We are unaware of any other publications measuring herbivory rates in the CRD, but high grazing is consistent with the results derived from stable isotopes, which indicate that shallow epipelagic particles fuel most of the zooplankton food web (Williams *et al.*, 2014).

Advective patterns for our study area suggest that waters upwelled at the center of the CRD, varying in location and intensity (Gutierrez-Rodriguez *et al.*, 2016; Landry *et al.*, 2016a; Selph *et al.*, 2016), with water parcels above the thermocline moving away from the dome. This pattern will lead to spatial variability that reflects the age of water parcels due to both advection away from the upwelling center and to cumulative production and consumption processes during transport. Interestingly, the minimum copepod in abundance occurred at the dome center (Fig. 5, Table IV). Low abundance of herbivorous copepods at the CRD center could be due to a variability in upwelling intensity leading to advection of surface dwelling organisms to areas away from the dome, to lags in reproductive response to enhanced phytoplankton production, a characteristic of many coastal upwelling systems (Miller, 2004), or to a combination of those two mechanisms. Lag times in reproductive response are consistent with low egg production of *Eucalanus inermis* at the dome cycles, and with higher egg production at Cycle 5 at the edge of the dome (Jackson and Smith, 2016). Other central CRD (Cycle 2) characteristics observed on our cruise were low phytoplankton growth rates (Selph *et al.*, 2016) and high picophytoplankton contribution to production (Fig. 7A), which suggests suboptimal conditions for mesozooplankton herbivory in the central dome region.

The stark difference in euphausiids/copepod patterns between the dome and the remaining cycles could be a consequence of distinct habitats within the vertical water column. Most herbivores in the CRD have been found to live generally in the shallow waters above the upper oxycline (Wishner *et al.*, 2013). The higher nighttime abundance of euphausiids (Table IV), suggests strong DVM, already shown in previous studies (Blackburn *et al.*, 1970; Brinton, 1979; Sameoto *et al.*, 1987). Strong DVM could increase their ability to keep position within the central dome region, by spending less time in fast moving surface waters and/or via return flows occurring at depth. Consistent with these findings, other authors have found high euphausiid abundances in the CRD compared with the adjacent oceanic provinces, contributing up to 35% of zooplankton biomass (Sameoto *et al.*, 1987). In this study, they accounted for 40% of nighttime biomass in Cycle 2 net tows. Sameoto *et al.* (Sameoto *et al.*, 1987) also found populations of common *Euphausia* spp. in deeper mesopelagic waters in the dome that did not exhibit DVM, suggesting that their diet consisted mainly of detritus, microzooplankton and other smaller zooplankton, fueled by production from the euphotic zone (Sameoto *et al.*, 1987). A low proportion of phytoplankton in the diets of larger euphausiids in this study was evident in the gut pigment contents of the 2–5 mm size class (Table V), which during Cycle 2 was equivalent to ~4% of body carbon day^{-1} and likely insufficient to sustain typical euphausiid metabolic needs at the temperatures (upper 40 m) of significant primary production (Brinton, 1979; Ross, 1982).

The resemblance between copepod and appendicularian relative patterns of abundance suggests that similar mechanisms, related to advection and/or distance from the dome center, affect these two groups of smaller, abundant zooplankton (Fig. 6). However, the proportional increase in appendicularian abundance between cycle groups was much larger than that observed for the copepod community. This is consistent with the high growth rates of pelagic tunicates (Bone, 2003). Cycle 2 numbers were comparable with those in the subtropical north Pacific (Landry *et al.*, 2008), but they increased by 5- (Cycles 3 and 4) to 10-fold (Cycle 1 and 5) in waters downstream of the dome. The fact that salps were detected in high abundances only in Cycle 5 is somewhat unexpected, although salps are well known for their patchy distributions and bursts of population growth (Bone, 2003; Madin *et al.*, 2006; Deibel and Lowen, 2012). It seems that Cycle 5, in the fast flowing NECC, was somewhat more conducive to community growth of mesozooplankton than the other "non-dome" cycles, given the combination of high new production seen in both nitrate uptake and net biogenic silica production (Krause *et al.*, 2016; Stukel *et al.*, 2016; Fig. 7C and B), and further confirmed by high egg production of *E. inermis* (Jackson and Smith, 2016) and higher grazing by smaller zooplankters (Figs 3A and 4B).

Table V: Average (± SE) percent (%) body carbon consumed per day (assuming a carbon composition of 0.4 DW) by mesozooplankton size fractionations during each experimental cycle

Size class (mm)	Cycle 1	Cycle 2	Cycle 3	Cycle 4	Cycle 5	Regional average
0.2	27.2 ± 5.3	11.4 ± 1.4	29.1 ± 9.7	17.4 ± 2.8	34.4 ± 6.4	23.7 ± 3.1
0.5	21.8 ± 3.4	15.0 ± 1.7	50.1 ± 11.9	19.0 ± 0.7	39.2 ± 2.3	29.5 ± 4.0
1	8.3 ± 0.9	8.3 ± 1.5	39.5 ± 4.7	14.9 ± 2.9	31.5 ± 3.9	21.1 ± 3.3
2	6.9 ± 3.2	4.2 ± 1.3	27.2 ± 3.7	11.3 ± 2.6	30.6 ± 14.6	16.5 ± 3.9
>5	0.6 ± 0.4	0.4 ± 0.5	2.2 ± 1.3	0.5 ± 0.5	2.8 ± 2.5	1.3 ± 0.6
Total community	15.3 ± 2.1	8.4 ± 0.5	31.9 ± 4.8	14.6 ± 1.9	30.2 ± 7.8	20.3 ± 2.6

Variability within the CRD

Despite the initial impression of uniformity in biomass standing stocks, our analysis of biomass spectra, grazing rates and taxonomic grouping reveal that the ETP zooplankton community is highly dynamic (Table I, Figs 3B, 4 and 5). Initially, we grouped the four oceanic cycles into "inside of the dome" (Cycles 2 and 4) with lower herbivory and larger organisms, and "outside of the dome" (Cycles 3 and 5), characterized by higher grazing and a community skewed toward smaller zooplankters (Fig. 4A and B). The coastal Cycle 1 was intermediate. However, this simple dichotomous grouping of cycles does not extend easily to patterns in diel migratory activity of the size-fractionated community or to variability observed in taxonomic composition (Table I, Figs 3A and 5). The dome cycles (Cycle 2 and 4) are similar in terms of their migrant structure, but Cycle 3 is also quite comparable (Fig. 3A), with lower total migrant biomass than the "dome cycles" but higher than Cycles 1 and 5 (Table I). Other similarities between Cycles 3 and 4, such as intermediate abundance of appendicularians and copepods (Fig. 5), support the idea of communities that vary with distance from the dome center.

One possible explanation for the observed variability is advection. However, simple advective transport without a concomitant increase in production implies that there must be other times (not observed in this study) when the abundances of copepod and appendicularians are just as high within the dome center (the source) as we observed in our cycles downstream of the dome. Given our observations, we suggest that changes in phytoplankton and mesozooplankton production along with physical advection result in compositional changes that lead to increases in herbivory (and zooplankton production) as water parcels move away from the dome center.

Compositional and trophic changes in zooplankton communities are known to occur elsewhere in waters advected away from upwelling centers. In the equatorial Pacific, for example, Timonin (Timonin, 1969) described zooplankton communities evolving in species dominance from herbivores to carnivores as waters moved away from the upwelling divergence. Similarly, in the same area, Décima *et al.* (Décima *et al.*, 2011) found that mesozooplankton grazing peaked about 1° latitude away from the upwelling, and Zhang *et al.* (Zhang *et al.*, 1995) found ingestion rates offset about 2−3° from the equator. While there are certain similarities between mesozooplankton communities in the CRD and equatorial upwelling systems, both in the ETP, there are also notable differences in biomass standing stocks and size spectra. These regional variations likely relate to their different characteristics in water-column stratification, current structure and micronutrient limitation. Using comparable methods to the current study, for example, Décima *et al.* (Décima *et al.*, 2011) found biomass values and grazing rates for the equatorial Pacific that were only a third to half those for the current CRD study, yet still ∼2 times higher than estimates for the same region measured a decade previously in the US JGOFS EqPac program (Dam *et al.*, 1995; Roman *et al.*, 1995; Zhang *et al.*, 1995). Zooplankton in the CRD thus appear to have substantially higher biomass and grazing impact than in the equatorial Pacific despite relatively similar levels of phytoplankton production, ∼1 g C m^{-2} day^{-1} (Landry *et al.*, 2016b; Landry *et al.*, 2011). One substantial ecosystem difference is the deep, less stratified euphotic zone in the equatorial region, which distributes significant production over the upper 100 m, rather than concentrating it in the upper 40 m. Thus, zooplankton of the CRD may be more efficient in directly exploiting the more concentrated phytoplankton production. In addition, as pointed out by Zhang *et al.* (Zhang *et al.*, 1995), the gut clearance rates derived during the EqPac cruises might have been lower than those of Dam and Peterson (Dam and Peterson, 1988) due to reduced food availability. Underestimation of grazing rates due to decreased prey abundance could potentially explain the mismatch in our data between mesozooplankton herbivory and production of large phytoplankton in the dome center area, which become more balanced as the community changes with distance from the dome (Fig. 7C).

Phytoplankton and grazing relationships

The lack of instantaneous relationships between phytoplankton and mesozooplankton is not surprising, given

the different time scales over which the assemblages respond to changes, from days to weeks, respectively. In fact, on a regional basis, production and grazing relationships were found to be roughly in balance for our cruise (Landry *et al.*, 2016b), though clearly not in daily balance at every location. However, the inverse relationship between mesozooplankton grazing and *Synechococcus* production (Fig. 7A), and for picophytoplankton generally (not shown), suggests that differences in the partitioning of primary production among phytoplankton size classes play an important role in the plankton community changes that occur away from the upwelling source. While we have noted *Synechococcus* in the guts of mesozooplankton in our PE measurements (Table III) and confirmed their presence in fecal pellets with microscopy (Stukel *et al.*, 2013), their contribution to mesozooplankton body carbon is marginal at best (Table III). This is consistent with the view that zooplankton energetic needs in the CRD must be supported more directly by significant production of larger phytoplankton (Tables II and V) and by microzooplankton.

The correlation between grazing and $bSiO_2$ is reasonable (Fig. 7B), but the consumption of diatoms alone is insufficient to explain the measured rates. We can estimate diatom carbon production (mean $\pm$ SD) in the "high grazing" cycles to be 18.2 ± 15.7 mg C m^{-2} day^{-1} for Cycle 3 and 29.4 ± 1.0 mg C m^{-2} day^{-1} for Cycle 5 based on $bSiO_2$ production and microscopy (Krause *et al.*, 2016; Taylor *et al.*, 2016), or a regional average of 31 mg C m^{-2} day^{-1} based on high-performance liquid chromatography pigments (Landry *et al.*, 2016b), which still only accounts for ~2–5% of the carbon consumed by mesozooplankton. This is atypical for an upwelling system, as indicated in a production-grazing balance analysis for the present cruise (Landry *et al.*, 2016b). Mesozooplankton could consume most, but not all, large phytoplankton production in two of the cycles, as estimates fall close to the 1:1 line between carbon consumption and production (Fig. 7C, no data for Cycle 1). However, efficient coupling between production and consumption by combined micro- and mesozooplankton grazers (Landry *et al.*, 2016b) is consistent with the observation of low export in the region (Stukel *et al.*, 2016), since little production is likely to sink unused out of the euphotic zone as fresh phyto-aggregates.

The cycle that falls notably below the 1:1 line is Cycle 2, with more excess production present in the dome cycle (Fig. 7C). One hypothesis explaining the pattern for Cycle 2 is that a substantial portion of "large phytoplankton" production was actually smaller than the 5-μm threshold typically considered for most copepods (Kleppel, 1993), probably in the 2–5 μm size range. However, another possibility is that the herbivorous component of the mesozooplankton community may not have been present in high enough densities to exert a significant grazing impact on the large autotrophs, as observed in fresh upwelled waters in the equatorial Pacific. Finally, given the caveats associated with Chl *a*-derived grazing estimates and our efforts to be conservative, it is possible we may have underestimated mesozooplankton consumption.

Our various grazing measurements, along with size and compositional changes in phytoplankton and zooplankton assemblages, suggest that continuous change with distance from the dome center might be a useful framework to describe change, similar to transitions observed in the equatorial open-ocean upwelling system (Timonin, 1969; Zhang *et al.*, 1995; Décima *et al.*, 2011). Subtle differences in the lower food web (Fig. 7A and B) could be significantly amplified by zooplankton trophic dynamics, resulting in substantial variability in community size-spectra, composition, grazing and potentially mesozooplankton production. While we can only speculate on the latter, the high percentages of mesozooplankton body carbon consumed (Table V) suggest production peaks at the edges of the CRD, consistent with the observed distributions of higher trophic level organisms that rely directly on plankton as prey or as indicators of high food areas (Ballance *et al.*, 2006; Vilchis *et al.*, 2006).

Finally, it is well established that microzooplankton can constitute an important portion of the diets of mesozooplankton (Gifford, 1991), and feeding on microzooplankton production could double our estimates of % carbon consumed (Calbet and Landry, 2004; Landry *et al.*, 2016b). The productive CRD resource environment is uniquely conducive to high mesozooplankton stocks, and we suspect that most of the primary production of the region flows either directly (as measured here) or indirectly (Landry *et al.*, 2016b; Stukel *et al.*, 2016) through them, ultimately fueling the higher trophic levels known to aggregate in the ETP.

DATA ARCHIVING

Mesozooplankton biomass and grazing estimates used in this manuscript are available from the Biological and Chemical Oceanography Data Management Office (http://www.bco-dmo.org/).

ACKNOWLEDGEMENTS

We thank the crew of the "R/V Melville" for all their wonderful work and help during our research cruise. Special thanks to Christina J. Bradley, Kate Tsyrklevich and Melanie Jackson for help with zooplankton sampling.

We also thank three anonymous reviewers whose comments improved the quality of this manuscript.

FUNDING

This component of the CRD FLUZiE study was supported by U.S. National Science Foundation grant OCE-0826626 to M.R.L. Additional support was provided by a NASA National Aeronautics and Space Administration, Earth and Space Science Fellowship to M.R.S.

REFERENCES

Acuna, J. L., Deibel, D., Saunders, P. A., Booth, B., Hatfield, E., Klein, B., Mei, Z. P. and Rivkin, R. (2002) Phytoplankton ingestion by appendicularians in the North Water. *Deep Sea Res. II*, **49**, 5101–5115.

Ballance, L. T., Pitman, R. L. and Fiedler, P. C. (2006) Oceanographic influences on seabirds and cetaceans of the eastern tropical Pacific: a review. *Prog. Oceanogr.*, **69**, 360–390.

Blackburn, M., Laurs, R. M., Owen, R. W. and Zeitzsch, B. (1970) Seasonal and areal changes in standing stocks of phytoplankton, zooplankton and micronekton in the eastern tropical Pacific. *Mar. Biol.*, **7**, 14–31.

Bochdansky, A. B., Deibel, D. and Hatfield, E. A. (1998) Chlorophyll a conversion and gut passage time for the pelagic tunicate *Oikopleura vanhoeffeni* (Appendicularia). *J. Plankton Res.*, **20**, 2179–2197.

Bone, Q. (2003) *The Biology of Pelagic Tunicates*. Oxford University Press, Oxford.

Brinton, E. (1979) Parameters relating to the distributions of planktonic organisms especially euphausiids in the eastern tropical Pacific. *Prog. Oceanogr.*, **8**, 125–189.

Calbet, A. and Landry, M. R. (2004) Phytoplankton growth, microzooplankton grazing, and carbon cycling in marine systems. *Limnol. Oceanogr.*, **49**, 51–57.

Conover, R. J., Durvasula, R., Roy, S. and Wang, R. (1986) Probable loss of chlorophyll-derived pigments during passage through the gut of zooplankton, and some of the consequences. *Limnol. Oceanogr.*, **31**, 878–887.

Dam, H. G. and Peterson, W. T. (1988) The effect of temperature on the gut clearance rate constant of planktonic copepods. *J. Exp. Mar. Biol. Ecol.*, **123**, 1–14.

Dam, H. G., Zhang, X. S., Butler, M. and Roman, M. R. (1995) Mesozooplankton grazing and metabolism at the equator in the central Pacific: implications for carbon and nitrogen fluxes. *Deep Sea Res. II*, **42**, 735–756.

Décima, M., Landry, M. R. and Rykaczewski, R. R. (2011) Broad scale patterns in mesozooplankton biomass and grazing in the eastern equatorial Pacific. *Deep Sea Res. II*, **58**, 387–399.

Deibel, D. and Lowen, B. (2012) A review of the life cycles and life history adaptations of pelagic tunicates to environmental conditions. *ICES J. Mar. Sci.*, **69**, 358–369.

Dore, J. E., Brum, J. R., Tupas, L. M. and Karl, D. M. (2002) Seasonal and interannual variability in sources of nitrogen supporting export in the oligotrophic subtropical North Pacific Ocean. *Limnol. Oceanogr.*, **47**, 1595–1607.

Durbin, E. G. and Campbell, R. G. (2007) Reassessment of the gut pigment method for estimating *in situ* zooplankton ingestion. *Mar. Ecol. Prog. Ser.*, **331**, 305–307.

Fernandez-Alamo, M. A. and Farber-Lorda, J. (2006) Zooplankton and the oceanography of the eastern tropical Pacific: a review. *Prog. Oceanogr.*, **69**, 318–359.

Fiedler, P. C. (2002) The annual cycle and biological effects of the Costa Rica Dome. *Deep Sea Res. I*, **49**, 321–338.

Franck, V. M., Smith, G. J., Bruland, K. W. and Brzezinski, M. A. (2005) Comparison of size-dependent carbon, nitrate, and silicic acid uptake rates in high- and low-iron waters. *Limnol. Oceanogr.*, **50**, 825–838.

Gifford, D. J. (1991) The protozoan-metazoan trophic link in pelagic ecosystems. *J. Protozool.*, **38**, 81–86.

Green, R. E. (1967) Relationship of thermocline to success of purse seining for tuna. *Trans. Am. Fish. Soc.*, **96**, 126–130.

Gutierrez-Rodriguez, A., Selph, K. E. and Landry, M. R. (2016) Phytoplankton growth and microzooplankton grazing dynamics across vertical environmental gradients determined by transplant *in situ* dilution experiments. *J. Plankton Res.*, **38**, 271–289.

Jackson, M. L. and Smith, S. L. (2016) Vertical distribution of Eucalanoid copepods within the Costa Rica Dome area of the Eastern Tropical Pacific. *J. Plankton Res.*, **38**, 305–316.

Kleppel, G. S. (1993) On the diets of calanoid copepods. *Mar. Ecol. Prog. Ser.*, **99**, 183–195.

Kleppel, G. S. and Pieper, R. E. (1984) Phytoplankton pigments in the gut contents of planktonic copepods from coastal waters off southern California. *Mar. Biol.*, **78**, 193–198.

Krause, J. W., Stukel, M. R., Taylor, A. G., Taniguchi, D. A., De Verneil, A. and Landry, M. R. (2016) Net biogenic silica production and the contribution of diatoms to new production and organic matter export in the Costa Rica Dome ecosystem. *J. Plankton Res.*, **38**, 216–229.

Landry, M. R., Décima, M., Simmons, M. P., Hannides, C. C. S. and Daniels, E. (2008) Mesozooplankton biomass and grazing responses to Cyclone *Opal*, a subtropical mesoscale eddy. *Deep Sea Res. II*, **55**, 1378–1388.

Landry, M. R., De Verneil, A., Goes, J. I. and Moffett, J. W. (2016a) Plankton dynamics and biogeochemical fluxes in the Costa Rica Dome: introduction to CRD Flux and Zinc Experiments. *J. Plankton Res.*, **38**, 167–182.

Landry, M. R., Selph, K. E., Decima, M., Gutierrez-Rodriguez, A., Stukel, M. R., Taylor, A. G. and Pasulka, A. L. (2016) Phytoplankton production and grazing balances in the Costa Rica Dome. *J. Plankton Res.*, **38**, 366–379.

Landry, M. R., Selph, K. E., Taylor, A. G., Decima, M., Balch, W. M. and Bidigare, R. R. (2011) Phytoplankton growth, grazing and production balances in the HNLC equatorial Pacific. *Deep Sea Res. II*, **58**, 524–535.

Longhurst, A. R. (1985) Relationship between diversity and the vertical structure of the upper ocean. *Deep Sea Res. I*, **32**, 1535–1570.

Madin, L. P., Kremer, P., Wiebe, P. H., Purcell, J. E., Horgan, E. H. and Nemazie, D. A. (2006) Periodic swarms of the salp *Salpa aspera* in the slope water off the NE United States: biovolume, vertical migration, grazing, and vertical flux. *Deep Sea Res. I*, **53**, 804–819.

Miller, C. B. (2004) *Biological Oceanography*. Blackwell Publishing, Malden, Oxford & Carlton, pp. i-ix, 1–402.

Pennington, J. T., Mahoney, K. L., Kuwahara, V. S., Kolber, D. D., Calienes, R. and Chavez, F. P. (2006) Primary production in the eastern tropical Pacific: a review. *Prog. Oceanogr.*, **69**, 285–317.

Roman, M. R., Dam, H. G., Gauzens, A. L., Urban-Rich, J., Foley, D. G. and Dickey, T. D. (1995) Zooplankton variability on the Equator at 140° W during the JGOFS EqPac Study. *Deep Sea Res. II*, **42**, 673–693.

Ross, R. M. (1982) Energetics of *Euphausia pacifica*. 2. Complete carbon and nitrogen budgets at 8°C and 12°C throughout the life span. *Mar. Biol.*, **68**, 15–23.

Saito, M. A., Rocap, G. and Moffett, J. W. (2005) Production of cobalt binding ligands in a *Synechococcus* feature at the Costa Rica upwelling dome. *Limnol. Oceanogr.*, **50**, 279–290.

Sameoto, D., Guglielmo, L. and Lewis, M. K. (1987) Day/night vertical distribution of euphausiids in the eastern tropical Pacific. *Mar. Biol.*, **96**, 235–245.

Sameoto, D. D. (1986) Influence of the biological and physical environment on the vertical distribution of mesozooplankton and micronekton in the eastern tropical Pacific. *Mar. Biol.*, **93**, 263–279.

Scott, M. D. and Cattanach, K. L. (1998) Diel patterns in aggregations of pelagic dolphins and tunas in the eastern Pacific. *Mar. Mammal Sci.*, **14**, 401–428.

Selph, K. E., Landry, M. R., Taylor, A. G., Gutierrez-Rodriguez, A., Stukel, M. R., Wokuluk, J. and Pasulka, A. L. (2016) Phytoplankton production and taxon-specific growth rates in the Costa Rica Dome. *J. Plankton Res.*, **38**, 199–215.

Shuman, F. R. and Lorenzen, C. J. (1975) Quantitative degradation of chlorophyll by a marine herbivore. *Limnol. Oceanogr.*, **20**, 580–586.

Stukel, M. R., Benitez-Nelson, C. R., Décima, M., Taylor, A. G. and Landry, M. R. (2015) The biological pump in the Costa Rica Dome: an open ocean upwelling system with high new production and low export. *J. Plankton Res.*, **38**, 348–365.

Stukel, M. R., Décima, M., Selph, K. E., Taniguchi, D. A. A. and Landry, M. R. (2013) The role of *Synechococcus* in vertical flux in the Costa Rica upwelling dome. *Prog. Oceanogr.*, **112**, 49–59.

Taylor, A. G., Landry, M. R., Freibott, A., Selph, K. E. and Gutierrez-Rodriguez, A. (2016) Patterns of microbial community biomass, composition and HPLC diagnostic pigments in the Costa Rica upwelling dome. *J. Plankton Res.*, **38**, 183–198.

Timonin, A. G. (1969) Structure of pelagic associations—quantitative relationship between different trophic groups of plankton in frontal zones of tropical ocean. *Oceanol. USSR*, **9**, 686–695.

Vilchis, L. I., Ballance, L. T. and Fiedler, P. C. (2006) Pelagic habitat of seabirds in the eastern tropical Pacific: effects of foraging ecology on habitat selection. *Mar. Ecol. Prog. Ser.*, **315**, 279–292.

Williams, R. L., Wakeham, S., Mckinney, R. and Wishner, K. F. (2014) Trophic ecology and vertical patterns of carbon and nitrogen stable isotopes in zooplankton from oxygen minimum zone regions. *Deep Sea Res. I*, **90**, 36–47.

Wishner, K. F., Outram, D. M., Seibel, B. A., Daly, K. L. and Williams, R. L. (2013) Zooplankton in the eastern tropical north Pacific: boundary effects of oxygen minimum zone expansion. *Deep Sea Res. I*, **79**, 122–140.

Wyman, M. (1992) An *in vivo* method for the estimation of phycoerythrin concentrations in marine cyanobacteria (*Synechococcus* spp.). *Limnol. Oceanogr.*, **37**, 1300–1306.

Zhang, X., Dam, H. G., White, J. R. and Roman, M. R. (1995) Latitudinal variations in mesozooplankton grazing and metabolism in the central tropical Pacific during the US JGOFS EqPac Study. *Deep Sea Res. II*, **42**, 695–714.